Linear response treatment of multipole excitations at finite temperature

F. Alasia, O. Civitarese, and M. Reboiro
Department of Physics, University of La Plata, (1900) La Plata, Argentina
(Received 5 May 1988)

Multipole excitations $\lambda^{\pi}=2^{+}$ and 3^{-}, in ^{116}Sn and ^{208}Pb, are calculated within the formalism of the finite-temperature linear response theory. Low- and high-energy strength distributions, for quadrupole and octupole vibrations, are shown as a function of the nuclear temperature. The resulting energy-weighted sum rules, for the associated multipole operators, are found to be weakly varying functions of the temperature T, in the interval $0 \leq T \leq 2$ MeV, provided off-diagonal blocks of the response matrix are included in the formalism.

I. INTRODUCTION

The study of temperature-dependent effects upon collective vibrations in finite nuclear systems has been presented in terms of the discrete random-phase approximations (RPA),[1–4] the coordinate representation method,[5] the functional representation method,[6] and in the semiclassical approximation.[7] The features that emerge from the above-mentioned references[1–7] are mostly related to the thermal collapse of low-lying vibrational states; an effect which is due to the thermal blocking of active configurations around the Fermi surface and to the shift and broadening of strength distributions for high-lying collective states, namely, for isoscalar and isovector giant resonances. A common difficulty associated with discrete temperature-dependent calculations of collective energies and strength distributions in finite nuclei is possed by the relatively large number of collective roots of the corresponding dispersion relations that have to be searched for in order to fulfill the relevant sum rules. In this respect, the adoption of techniques, other than discrete RPA calculations at finite temperature, seems to be more adequate. Concerning this problem, an alternative description has been proposed in Ref. 8, which is based on perturbative techniques. Another description, based on the Bethe-Salpeter equation,[9,10] has been proposed for the description of strength distributions in deformed nuclei at finite temperature. The case of multiple excitations in highly excited deformed systems[10] provides us with a definite example about the suitability of the method. In this paper we are going to discuss the application of linear response techniques in conjunction with Bethe-Salpeter's equation method to the description of multipole vibrations in spherical systems. The equations of motion are solved for quadrupole and octupole fields for the case of a separable multipole interaction.[11] We have adopted this very simple force, which nevertheless has been shown to reproduce fairly well the observed features of quadrupole and octupole vibrational fields,[11] in order to show some differences between the present and previously reported results based on discrete RPA treatments of the same interactions.[1] At the same time it is our aim to show that the present treatment appears to be more reliable than the discrete RPA one, when huge dimensions of pair configurations are required, i.e., for finite temperatures. The paper is organized in the following manner: theoretical details of the formalism are discussed in Sec. II. Results for multipole vibrations $\lambda^{\pi}=2^{+}$ and 3^{-} for a superfluid nucleus ^{116}Sn and for a normal one ^{208}Pb are discussed in Sec. III. Conclusions are drawn in Sec. IV.

II. FORMALISM

In this section we are going to discuss the formalism which is based on the finite-temperature treatment of the single-particle and multipole-multipole terms of the model Hamiltonian[11]

$$\hat{H}=\sum_{j,t_z(n,p)} \varepsilon_j(t_z)\hat{a}_j^{\dagger}(t_z)\hat{a}_j(t_z) - \frac{1}{2}\sum_{\substack{\lambda\mu \\ t_z,t_{z'}}} \varkappa_{\lambda}(t_z;t_{z'})\hat{Q}_{\lambda\mu}^{\dagger}(t_z)\hat{Q}_{\lambda\mu}(t_{z'}) , \quad (1)$$

where we have used the standard notation.[3,11] Temperature-dependent effects can be accounted for by introducing single-particle occupation numbers[1]

$$n_{j,t_z}(T)=(1+\exp\{[\epsilon_j(t_z)-\mu_F(t_z)]/T\})^{-1} , \quad (2)$$

where T is the nuclear temperature, expressed in energy units, associated to a given excitation energy of the nucleus and $\mu_F(t_z)$ is the Fermi energy obtained from number conservation conditions at finite temperature. Matrix elements $q_{\lambda}(p_z,p_1,t_z)$ of the multipole operator $\hat{Q}_{\lambda\mu}(t_z)$ are defined by

$$q_{\lambda}(p_2,p_1,t_z)=\frac{1}{1+\delta(p_2,p_1)}\left[\frac{\langle p_2\|Q_{\lambda\mu}\|p_1\rangle}{2\lambda+1}\right] , \quad (3)$$

where (p_1,p_2) denotes a configuration of two single-particle states which can be coupled to angular momentum λ; $\delta(p_2,p_1)$ is a Kroenecker delta symbol and double bars stand for reduced matrix elements.[12] The matrix elements of the separable multipole-multipole residual interaction, which appears in Hamiltonian (1), can be written as

 ©1989 The American Physical Society

$$H_{\text{int}}\{[j_2(t_{z'})j_1(t_{z'})]_{\lambda\mu'}[k_2(t_z)k_1(t_z)]_{\lambda\mu}\} = -\delta_{\mu,\mu'}\chi(t_z;t_{z'})q_\lambda(j_2j_1;t_{z'})q_\lambda(k_2k_1;t_z) \ . \tag{4}$$

The finite-temperature random-phase-approximation (FTRPA) treatment of the Hamiltonian (1) has been described in detail in Ref. 3 where the vibrational spectrum of FTRPA phonons has been obtained by solving the corresponding secular equation for a discrete number of configurations $[p_2(t_z),p_1(t_z)]_{\lambda\mu}$. This procedure can be attempted, provided a moderate number of particle-hole configurations are included in the zero-temperature case. As soon as the temperature increases, since single-particle states will be distributed with occupation numbers (2), restrictions over the particle-hole character of the $[p_2(t_z),p_1(t_z)]_{\lambda\mu}$ pair, namely, $p_2 \geq p_{\text{Fermi}}$, $p_1 < p_{\text{Fermi}}$, will no longer be operative. It means that for finite temperature all configurations of the type $[p_2(t_z),p_1(t_z)]_{\lambda\mu}$ with $p_2(t_z) \geq p_1(t_z)$ ought to be included. Therefore, the number of configurations itself will be a function of the temperature T due to the fact that a given $[p_2(t_z),p_1(t_z)]_{\lambda\mu}$ pair will be suppressed from the configuration space only if the associated factor

$$n_{p_1,t_z}(T) - n_{p_2,t_z}(T) \tag{5}$$

vanishes.[3] Calculations based on this scheme are feasible but the search for FTRPA frequencies becomes cumbersome because of the large number of configurations which have to be included, and also for numerical instabilities which could show up due to the fact that considerable large numbers of unperturbed pair energies $\epsilon_{p_1}(t_z) - \epsilon_{p_2}(t_z)$ could differ in a small amount. In order to overcome this problem we shall work in the framework of the linear response theory[9] extended to finite temperature. Let us briefly review the zero-temperature case in order to introduce some formulas which are relevant for the finite-temperature case. Linear response equations for the particle-hole channel of the RPA density matrix in the presence of an external field f can be written as[9]

$$\left[\begin{bmatrix} A & B \\ B^* & A^* \end{bmatrix} - \hbar\omega \begin{bmatrix} I & 0 \\ 0 & -I \end{bmatrix}\right] \begin{bmatrix} \rho^{(1)ph} \\ \rho^{(1)hp} \end{bmatrix} = - \begin{bmatrix} f^{ph} \\ f^{hp} \end{bmatrix} , \tag{6}$$

where A and B are the usual RPA matrices[9] and ω are the frequencies associated to the external field. The solutions of the inhomogeneous Eq. (6) can be written in terms of the solutions of the homogeneous RPA equations

$$S\chi = \eta\chi\hbar\Omega \ , \tag{7}$$

where

$$S = \begin{bmatrix} A & B \\ B^* & A^* \end{bmatrix}, \quad \chi = \begin{bmatrix} X & Y^* \\ Y & X^* \end{bmatrix}, \quad \eta = \begin{bmatrix} I & 0 \\ 0 & -1 \end{bmatrix} . \tag{8}$$

The matrices χ and Ω are the eigenvector and positive and negative eigenvalue matrices, respectively, for a vanishing external field. With these definitions the inhomogeneous equations can be written

$$(S - \hbar\omega\eta)\rho^{(1)} = -f \ . \tag{9}$$

Writing $S = \eta\chi\hbar\Omega\chi^\dagger$ and replacing it in (9) we obtain

$$\hbar[\eta\chi(\Omega-\omega)\eta\chi^\dagger\eta]\rho^{(1)} = -f \ . \tag{10}$$

By matrix inversion Eq. (10) takes the form

$$\rho^{(1)}_{kk'} = \sum_{jj'} R_{kk',jj'}(\omega) f_{jj'} \ , \tag{11}$$

where

$$R(\omega) = \frac{1}{\hbar}[\chi(\omega-\Omega)^{-1}\eta\chi^\dagger]$$

is the linear response matrix which, in terms of the forward- and backward-going amplitudes X and Y, respectively, has matrix elements of the form

$$R(\omega)_{kk',jj'} = \frac{1}{\hbar}\sum_{\nu>0}\left[\frac{X^\nu(kk')X^\nu(jj')^*}{\omega-\Omega_\nu} - \frac{Y^\nu(kk')Y^\nu(jj')^*}{\omega+\Omega_\nu}\right] . \tag{12}$$

The extension of the above discussed formulas to finite temperature can be straightforwardly performed introducing a diagonal matrix with the occupation factors (5)

$$\tau = \begin{bmatrix} [n_{j_1}(T) - n_{j_2}(T)] & & \\ & \ddots & \\ & & -[n_{j_1}(T) - n_{j_2}(T)] \end{bmatrix} . \tag{13}$$

After some algebra we obtain

$$R_T(\omega)_{kk',jj'} = \frac{1}{\hbar}\sum_{\nu>0}\left[\frac{X^\nu(kk')X^\nu(jj')^*}{\omega-\Omega_\nu} - \frac{Y^\nu(kk')Y^\nu(jj')^*}{\omega+\Omega_\nu}\right]_T \times [n_j(T) - n_{j'}(T)] \ . \tag{14}$$

Equation (13) can also be written in terms of the unperturbed linear response matrix

$$R^0_T(\omega)_{kk',jj'} = \delta_{kj}\delta_{k'j'}[n_{j'}(T) - n_j(T)] \times \left[\frac{1}{\omega-\epsilon_k+\epsilon_{k'}+i\eta} - \frac{1}{\omega+\epsilon_k+\epsilon_{k'}+i\eta}\right] \tag{15}$$

using the linearized Bethe-Salpeter equation

$$R_T(\omega)_{pq,p'q'} = R^0_T(\omega)_{pq,p'q'} + \sum_{\substack{p_1,q_1 \\ p_2,q_2}} R^0_T(\omega)_{pq,p_1q_1} H_{\text{int}}(p_1q_1,p_2q_2) \times R_T(\omega)_{p_2q_2,p'q'} \ . \tag{16}$$

Replacing $H_{\text{int}}(pq,p'q')$ by its value, Eq. (4) in Eq. (16), and defining

$$R_T(\omega)_{t_z;t_{z'}}=\sum_{\substack{(p_2\geq p_1)_{t_z}\\(q_2\geq q_1)_{t_{z'}}}} q_\lambda(\bar{p}_2p_1;t_z)R_T(\omega)_{p_2p_1,q_2q_1}\times q_\lambda(\bar{q}_2q_1;t_{z'}) , \tag{17}$$

we finally obtain the matrix equation

$$R_T(\omega)_{t_z;t_{z'}}=R_T^0(\omega)_{t_z;t_{z'}}-\sum_{t_{z_1},t_{z_2}} R_T(\omega)_{t_{z_1};t_{z_2}}R_T^0(\omega)_{t_z;t_{z_1}}R_T(\omega)_{t_{z_2};t_{z'}} , \tag{18}$$

where the matrix $R_T^0(\omega)_{t_z;t_{z'}}$, which is given by Eq. (17) replacing $R_T(\omega_2)_{p_2p_1,q_2q_1}$ by the matrix elements $R_T^0(\omega)_{p_2p_1,q_2q_1}$, cf. Eq. (18), denotes both proton and neutron configurations. We are, at this point, dealing with a coupled system of matrices of the form

$$\begin{aligned}
R_T(\omega)_{nn}&=R_T^0(\omega)_{nn}\\
&\quad-[\varkappa_{nn}R_T^0(\omega)_{nn}+\varkappa_{pn}R_T^0(\omega)_{np}]R_T(\omega)_{nn}\\
&\quad-[\varkappa_{np}R_T^0(\omega)_{nn}+\varkappa_{pp}R_T^0(\omega)_{np}]R_T(\omega)_{pn} ,\\
R_T(\omega)_{np}&=R_T^0(\omega)_{np}\\
&\quad-[\varkappa_{nn}R_T^0(\omega)_{nn}+\varkappa_{pn}R_T^0(\omega)_{np}]R_T(\omega)_{np}\\
&\quad-[\varkappa_{np}R_T^0(\omega)_{nn}+\varkappa_{pp}R_T^0(\omega)_{np}]R_T(\omega)_{pp} ,\\
R_T(\omega)_{pp}&=R_T^0(\omega)_{pp}\\
&\quad-[\varkappa_{np}R_T^0(\omega)_{pn}+\varkappa_{pp}R_T^0(\omega)_{pp}]R_T(\omega)_{pp}\\
&\quad-[\varkappa_{nn}R_T^0(\omega)_{pn}+\varkappa_{pn}R_T^0(\omega)_{pp}]R_T(\omega)_{np} ,\\
R_T(\omega)_{pn}&=R_T^0(\omega)_{pn}\\
&\quad-[\varkappa_{nn}R_T^0(\omega)_{pn}+\varkappa_{pn}R_T^0(\omega)_{pp}]R_T(\omega)_{nn}\\
&\quad-[\varkappa_{np}R_T^0(\omega)_{pn}+\varkappa_{pp}R_T^0(\omega)_{pp}]R_T(\omega)_{pn} .
\end{aligned} \tag{19}$$

After performing some algebra and remembering that $R_T^0(\omega)_{pn}=R_T^0(\omega)_{np}=0$, we obtain

$$\begin{aligned}
R_T(\omega)_{nn}&=\frac{[1+\varkappa_{pp}R_T^0(\omega)_{pp}]R_T^0(\omega)_{nn}}{[1+\varkappa_{nn}R_T^0(\omega)_{nn}][1+\varkappa_{pp}R_T^0(\omega)_{pp}]-\varkappa_{np}^2R_T^0(w)_{nn}R_T^0(\omega)_{pp}} ,\\
R_T(\omega)_{np}&=\frac{-\varkappa_{np}R_T^0(\omega)_{nn}R_T^0(\omega)_{pp}}{[1+\varkappa_{nn}R_T^0(\omega)_{nn}][1+\varkappa_{pp}R_T^0(\omega)_{pp}]-\varkappa_{np}^2R_T^0(w)_{nn}R_T^0(\omega)_{pp}} ,\\
R_T(\omega)_{pp}&=\frac{[1+\varkappa_{nn}R_T^0(\omega)_{nn}]R_T^0(\omega)_{pp}}{[1+\varkappa_{nn}R_T^0(\omega)_{nn}][1+\varkappa_{pp}R_T^0(\omega)_{pp}]-\varkappa_{np}^2R_T^0(w)_{nn}R_T^0(\omega)_{pp}} ,\\
R_T(\omega)_{pn}&=\frac{-\varkappa_{np}R_T^0(\omega)_{nn}R_T^0(\omega)_{pp}}{[1+\varkappa_{nn}R_T^0(\omega)_{nn}][1+\varkappa_{pp}R_T^0(\omega)_{pp}]-\varkappa_{np}^2R_T^0(w)_{nn}R_T^0(\omega)_{pp}} .
\end{aligned} \tag{20}$$

Equation (20) defines the block elements of the linear response matrix in neutron-neutron, proton-proton, and neutron-proton channels, and can also be written in terms of isoscalar and isovector components of the multipole operator $Q_{\lambda\mu}$, namely,

$$\begin{aligned}
Q_{\lambda\mu}(\tau=0)&=\frac{1}{\sqrt{2}}[Q_{\lambda\mu}(n)+Q_{\lambda\mu}(p)] ,\\
Q_{\lambda\mu}(\tau=1)&=\frac{1}{\sqrt{2}}[Q_{\lambda\mu}(n)-Q_{\lambda\mu}(p)] .
\end{aligned} \tag{21}$$

Thus the corresponding isoscalar and isovector linear response matrices can be written as

$$\begin{aligned}
R_T(\omega,\tau=0)&=\tfrac{1}{2}[R_T(\omega)_{nn}+R_T(\omega)_{pp}+R_T(\omega)_{np}+R_T(\omega)_{pn}] ,\\
R_T(\omega,\tau=1)&=\tfrac{1}{2}[R_T(\omega)_{nn}+R_T(\omega)_{pp}-R_T(\omega)_{np}-R_T(\omega)_{pn}] ,
\end{aligned} \tag{22}$$

respectively. Therefore, the information concerning strength distributions of multipole excitations can be extracted from the imaginary part of the linear response matrix, i.e.,

$$\begin{aligned}
S(\lambda^\pi,\omega,\tau)&=-\frac{1}{\pi}\mathrm{Img}R_T(\lambda^\pi,\omega,\tau) ,\\
S_E(\lambda^\pi,\tau)&=\int_0^\infty d\omega\,\omega S(\lambda^\pi,\omega,\tau) ,
\end{aligned} \tag{23}$$

which are the strength distributions and the integrated energy-weighted strength, respectively, of the multipole field λ^π.

III. RESULTS AND DISCUSSION

In this section we are going to present the results of our calculations of the finite temperature linear response for multipole excitations in ^{116}Sn and ^{208}Pb. We have selected these nuclei since they are good examples of superfluid and normal systems, respectively.

For the single-particle basis we have chosen spherical Nilsson's energy levels and wave functions up to seven shells for ^{116}Sn, and up to nine shells for ^{208}Pb. The corresponding coupling constants, $k_n=0.0638$, $\mu_n=0.0319$,

$k_p=0.0674$, $\mu_p=0.0382$ for ^{116}Sn and $k_n=0.0636$, $\mu_n=0.0233$, $k_p=0.0604$, $\mu_p=0.0379$ for ^{208}Pb, have been adjusted in order to reproduce observed single-particle energy sequences for active orbits near closed shells.[13]

We have evaluated multipole excitations with $\lambda^\pi=2^+$ and 3^- in both nuclei. For finite-temperature values T, within the interval $0\leq T\leq 2$ MeV, we have calculated single-particle occupations numbers with and without the inclusion of pairing correlations[1] for ^{116}Sn and ^{208}Pb, respectively. The critical temperature associated with the collapse of the neutron-pairing gap for ^{116}Sn was found to be of the order of $T_c=0.6$ MeV. This result is consistent with previously reported calculations about the temperature response of the quasiparticle mean field.[14]

Results corresponding to the unperturbed linear response, Eqs. (15) and (23), are shown in Figs. 1 and 2. In these figures the function

$$S^{(0)}(\lambda^\pi,\omega,T)=(-1/\pi)\mathrm{Im}[R_T^{(0)}(\lambda^\pi,\omega,T]$$

is shown, for each multipolarity and different values of the temperature, for protons and neutrons, separately. It should be noted that $S^{(0)}(\lambda^\pi,\omega,T)$ is a distribution function associated with the non-energy-weighted strength distribution, and the total energy-weighted strength can readily be obtained from it by integration, as it has been defined in Eq. (23). The same notation has been employed in Figs. 3 and 4 where the results corresponding to the perturbed linear response are shown, as we shall discuss later on. In obtaining the results which are shown in Figs. 1–4, we have adopted a value $\eta=1$ MeV for the parameter introduced in Eq. (15). This value is similar to that of Ref. 8. Since with η we are averaging over isolated pair configurations, in such a way that the energy denominators of Eq. (15) do not diverge, we have performed calculations for several values of η until resonances around unperturbed pair energies, of the particle-hole or two quasiparticles configurations, were washed out. The final value for η, i.e., $\eta=1$ MeV, was adopted by following this procedure. As can be observed from the results shown in Figs. 1 and 2, the unperturbed linear response is nearly independent of T, except for the low-energy domain in ^{116}Sn where the collapse of the pairing gap produces the blocking of some neutron pair configurations. The dominance of $\Delta N=2$ configurations for $\lambda^\pi=2^+$ and $\Delta N=1$ and 3 for $\lambda^\pi=3^-$ states is clearly observed, both in ^{116}Sn and in ^{208}Pb.

In order to illustrate the convenience of the present approach, with respect to the usual one, namely, the discrete sum over configurations, let us indicate that for the case of ^{208}Pb at $T=0$ we are dealing with 204 configurations for $\lambda^\pi=3^-$, and with 96 configurations for $\lambda^\pi=2^+$, while at $T=2$ MeV the number of configurations are 584 and 371, respectively. For ^{116}Sn, at $T=0$, we have 164 and 98 configurations for octupole and quadrupole excitations, and at $T=2$ MeV the number of unperturbed states increases to 351 and 228, respectively. The advantage possessed by the linear response treatment becomes evident since with the same basis we have to compute the correlated strength distri-

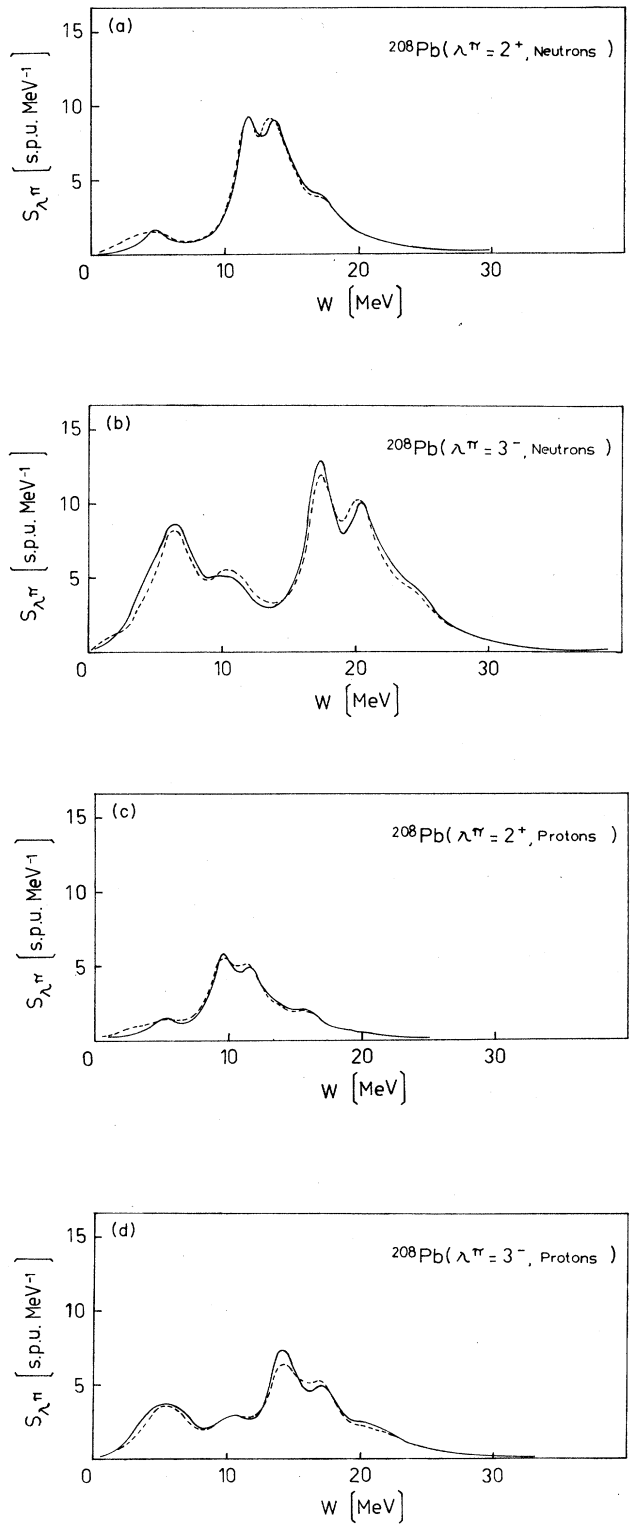

FIG. 1. Unperturbed strength distributions for multipole excitations $\lambda^\pi=2^+$ and 3^- in ^{208}Pb. The distribution function for multipole transitions corresponding to neutron-neutron and proton-proton configurations are shown for zero temperature (solid lines) and for $T=2$ MeV (dashed lines), as a function of the excitation energy ω.

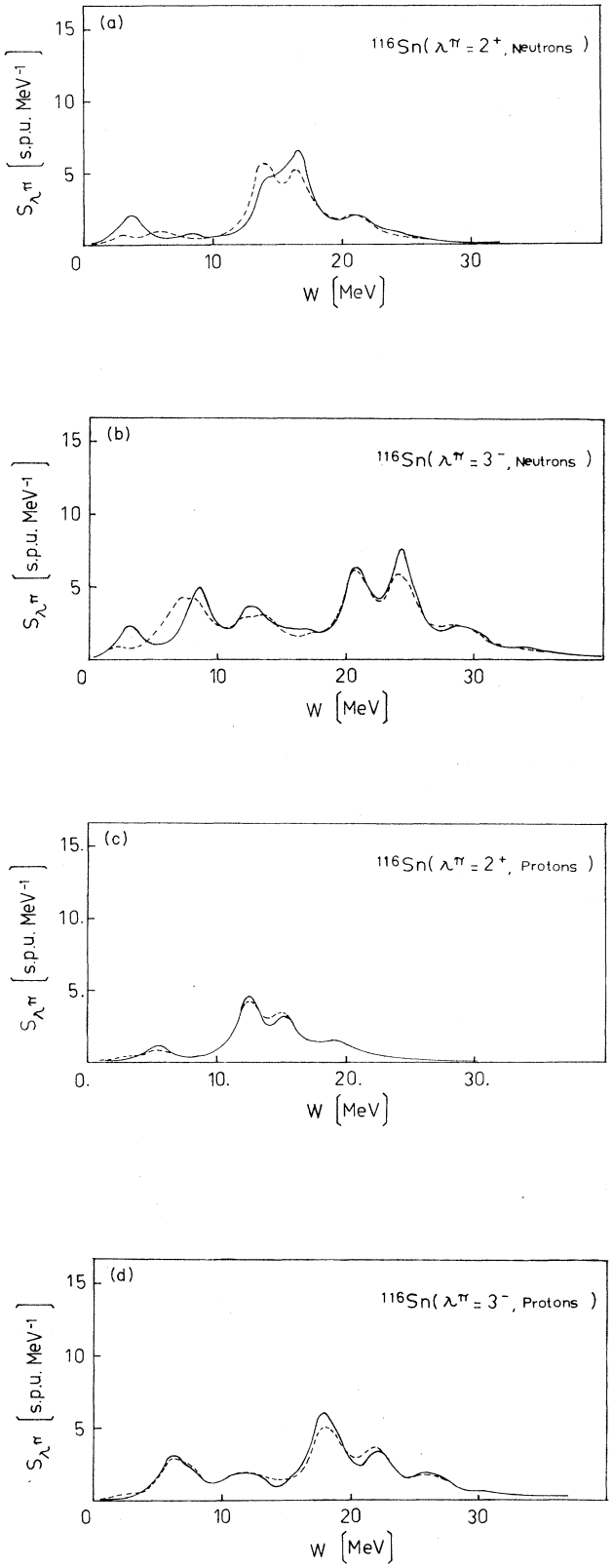

FIG. 2. Unperturbed strength distributions for multipole excitations $\lambda^{\pi}=2^{+}$ and 3^{-} in ^{116}Sn. The results are shown with the same notation used in Fig. 1.

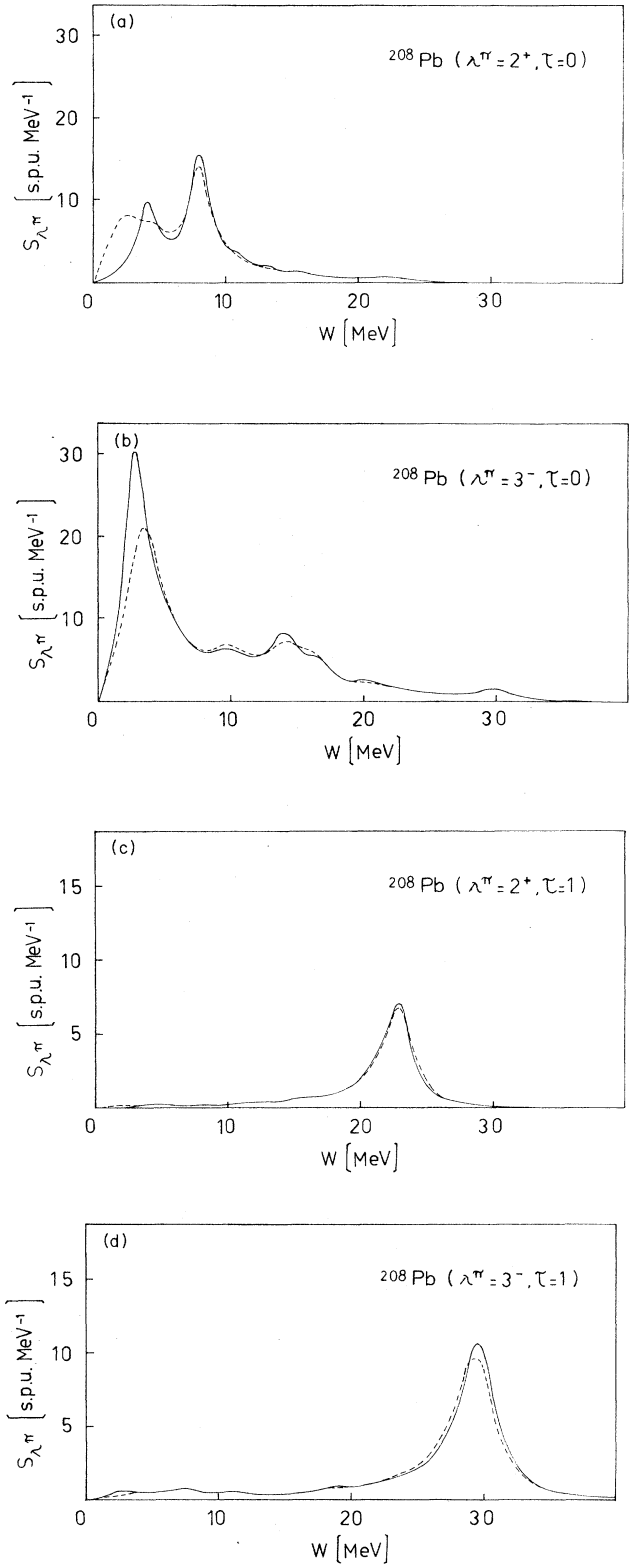

FIG. 3. Strength distributions for multipole isoscalar ($\tau=0$) and isovector ($\tau=1$) transitions in ^{208}Pb. Quadrupole ($\lambda^{\pi}=2^{+}$) and octupole ($\lambda^{\pi}=3^{-}$) temperature-dependent linear-response functions are shown for $T=0$ (solid lines) and for $T=2$ MeV (dashed lines).

butions for quadrupole and octupole states. In order to get some confidence on the $T=0$ results for the perturbed case, we have done two different sets of calculations, namely, with a conventional RPA code[15] and with the present one based on the linear response theory of Sec. II. The results of both calculations coincide for the location of the discrete roots and for the centroids of the strength distributions, as well as for the $B(E\lambda)$ and multipole moments for low-lying and high-lying isoscalar and isovector resonances. We have used the following set of coupling constants, which are given in units of MeV fm$^{-2\lambda}$: $\chi(0)=0.429\times10^{-3}$, $\chi(1)=-0.156\times10^{-2}$ for quadrupole vibrations in ^{208}Pb; $\chi(0)=0.640\times10^{-5}$, $\chi(1)=-0.291\times10^{-4}$ for octupole vibrations in ^{208}Pb; $\chi(0)=0.191\times10^{-2}$, $\chi(1)=-0.676\times10^{-2}$ for quadrupole vibrations in ^{116}Sn; $\chi(0)=0.413\times10^{-4}$, $\chi(1)=-0.187\times10^{-3}$ for octupole states in ^{116}Sn, respectively. With $\chi(0)$ and $\chi(1)$ we have denoted isoscalar coupling constants and the obtained energies for the first excited states $\omega(\lambda_1^\pi)$ are the following: $\omega(2^+,{}^{208}\text{Pb})=4.086$ MeV, $\omega(3^-,{}^{208}\text{Pb})=2.614$ MeV, $\omega(2^+,{}^{116}\text{Sn})=1.293$ MeV, $\omega(3^-,{}^{116}\text{Sn})=2.266$ MeV, respectively. We have also verified that within a 5% accuracy the corresponding energy-weighted sum rules exhausted the model-independent values.[16]

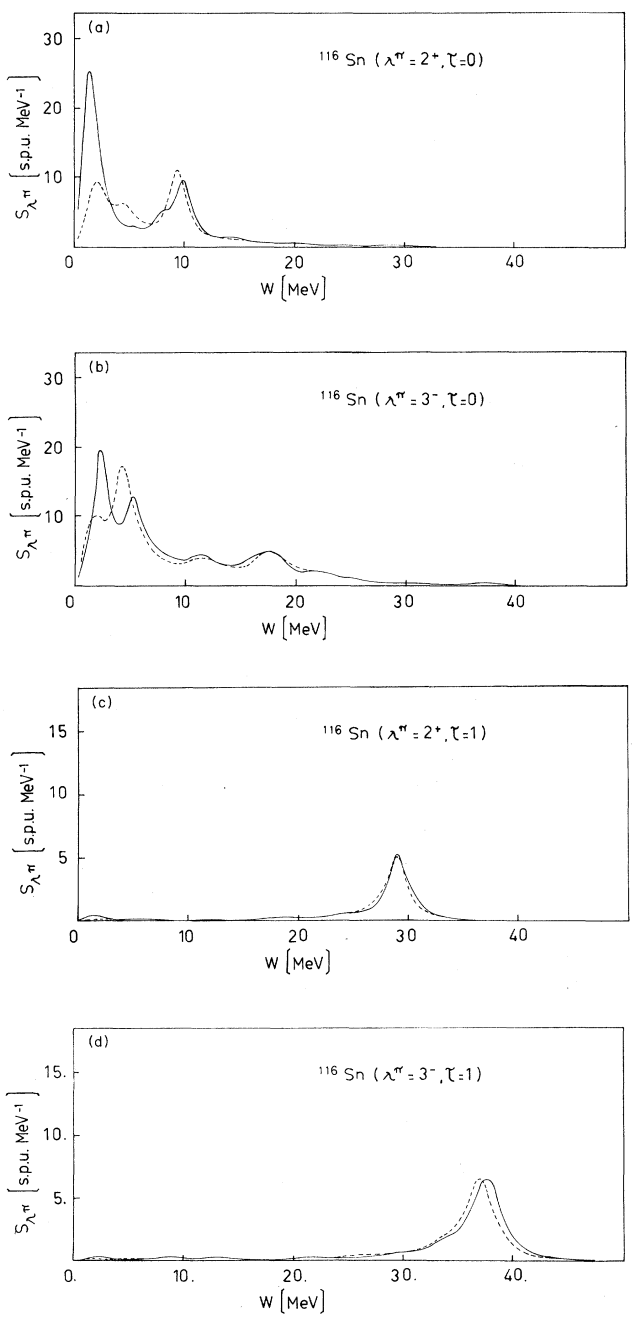

FIG. 4. Strength distribution functions for multipole fields in ^{116}Sn. The results are indicated with the same notation used in Fig. 1.

In constructing the matrix elements of the linear response matrix, at a given temperature T, all possible pair configurations have been included without an energy cutoff. For the single-particle states it means that, for each temperature, they were always thermal occupied states in the high-energy region of the spectrum. We have also tested the stability of our results by increasing the number of single-particle states. The final set, which has been mentioned before, gave us stable results for the unperturbed sum rules as compared to the model-independent values.

Results corresponding to energy-weighted sum rules (EWSR) for quadrupole and octupole excitations in ^{116}Sn and ^{208}Pb are shown in Table I. The model-independent EWSR for neutrons and protons, shown in Table I, have been calculated using Bohr and Mottelson's[16] formulas, but perform explicitly the radial integrals associated to each multipole moment. It should be noted that for the finite-temperature case approximations based on a series expansion of the radial integrals in terms of the (a/R) ratio[12] are no longer valid, as we have found from the results of our calculations. The results which are displayed in Table I show that the temperature dependence of the linear response EWSR is less pronounced than the one reported from results based on discrete RPA calculations.[1–4] The difference could be attributed to numerical uncertainties in the search of RPA roots at finite T, which are difficult to avoid.

Centroids and widths for isoscalar and isovector energy-weighted strength distributions are shown in Table II. The corresponding strength functions are shown in Figs. 3 and 4. From the results which are displayed in Table II we can observe a moderate shift upwards for the isoscalar energy-weighted sum rules, and downwards for the isovector energy-weighted sum rules for increasing values of T. At the same time, the spreading width of both modes increases for larger T values. Both features, namely the energy shift and the broadening of the spreading width, could be traced back to the occurrence of thermal blocking effects induced by changes in thermal occupation factors. These effects are more pronounced for low-lying $\Delta N=0$ and $\Delta N=1$ transitions, for quadrupole and octupole excitations, respectively. However, since at finite T the number of particle-

TABLE I. Energy-weighted sum rules for multipole operators $\hat{Q}_{\lambda\mu}$ with $\lambda^\pi=2^+$ and 3^- in ^{208}Pb and ^{116}Sn. Neutron [EWSR(n)], proton [EWSR(p)], isoscalar [EWSR($\tau=0$)], and isovector [EWSR($\tau=1$)] values are displayed as a function of the temperature T. The third and fourth columns show the unperturbed values which have been obtained by performing explicitly, at finite temperature, the corresponding radial integrals of the model-independent sum rules (Ref. 16). The fifth to eighth columns show the results obtained with the linear response matrix. All values are given in single-particle units [s.p.u.].

		Model-independent values		Correlated values			
λ^π	T (MeV)	EWSR(n)	EWSR(p)	EWSR(n)	EWSR(p)	EWSR($\tau=0$)	EWSR($\tau=1$)
				^{208}Pb			
2^+	0.0	930	530	950	462	706	705
	1.0	939	534	954	466	710	709
	2.0	948	543	959	467	713	712
3^-	0.0	2466	1224	2442	1029	1738	1733
	1.0	2485	1239	2432	1019	1728	1723
	2.0	2538	1282	2384	994	1693	1688
				^{116}Sn			
2^+	0.0	757	496	744	446	596	594
	1.0	719	497	710	446	579	577
	2.0	724	503	707	450	580	578
3^-	0.0	2075	1200	1735	1044	1394	1385
	1.0	1901	1206	1656	1041	1352	1344
	2.0	1934	1243	1605	1024	1319	1391

particle and hole-hole–like transitions increases and due to the fact that they are generally less energetic than the particle-hole transitions, the number of correlated low-lying states could increase. This is the reason for the broadening of the linear response for isoscalar quadrupole transitions in ^{208}Pb, as well as in ^{116}Sn. By the other side, contributions to the high-lying resonances, both for isoscalar and isovector transitions, are almost unaffected by the increase of the temperature apart from the small shift already mentioned before. These results are again showing some differences with respect to the results obtained within the discrete RPA approach. Insofar as our results are concerned, the thermal dependence of the multipole linear response is rather weak, except for quadrupole and octupole isoscalar strength distributions in ^{116}Sn. Consequently, it could be concluded that some of the commonly accepted arguments in favor of more significant changes in the vibrational features of nuclear modes at finite temperature, i.e., a broadening of the resonances with a clear linear dependence upon T,[1] would be only valid within the more restricted scope of the discrete first RPA description. The same conclusion could be valid for other temperature-dependent properties, i.e., changes in the nuclear radius determined from thermal

TABLE II. Energy centroids ($\bar{E}$), second moments (σ), energy maxima (E_{max}), and width (Γ) of the energy-weighted strength distributions corresponding to isoscalar ($\tau=0$) and isovector ($\tau=1$) multipole excitations ($\lambda^\pi=2^+$ and 3^-) in ^{208}Pb and ^{116}Sn are shown as a function of the temperature T. All values are given in MeV.

			^{208}Pb				^{116}Sn			
λ^π	τ	T	$\bar{E}$	σ	E_{max}	Γ	$\bar{E}$	σ	E_{max}	Γ
2^+	0	0.0	11.87	8.32	9.88	2.47	11.60	7.40	8.09	2.21
		1.0	11.89	7.91	9.40	2.09	11.45	7.50	8.05	2.28
		2.0	11.85	7.90	9.42	2.11	11.36	7.58	8.02	2.47
	1	0.0	28.87	5.21	28.99	2.41	22.71	5.29	22.90	2.84
		1.0	28.58	5.14	28.98	2.25	22.72	5.31	22.91	2.90
		2.0	28.61	5.15	29.04	2.29	22.72	5.34	22.90	3.02
3^-	0	0.0	16.94	9.88	18.01	6.11	15.57	9.31	14.06	8.71
		1.0	16.93	9.67	17.71	4.49	15.65	9.23	14.17	9.20
		2.0	16.95	9.67	17.92	6.05	15.75	9.18	14.56	9.84
	1	0.0	36.10	6.06	37.66	3.55	28.66	6.02	29.66	3.39
		1.0	35.78	6.04	37.06	3.41	28.60	5.99	29.06	3.58
		2.0	35.50	6.11	36.87	3.24	28.43	6.00	29.45	3.83

variations in the EWSR or the softening of nuclear vibrations determined from temperatures-dependent RPA frequencies.[1]

IV. CONCLUSIONS

We have shown that the linear response method can be applied to the calculation of strength distributions associated with multipole excitations at finite temperature. Temperature-dependent properties of these collective modes, such as shifts in the energy distributions of EWSR and the broadening of giant resonances modes, have been found to be less affected by thermal excitations than in previously reported works[1] based on the discrete RPA method. This difference in the thermal behavior of multipole strength distributions could be attributed, in the case of a conventional RPA method, to the onset of numerical instabilities in the search of a very large number of collective and noncollective roots of the temperature-dependent equation of motion. These numerical instabilities do not affect the results of the finite-temperature linear response method which appears to be more convenient than the standard RPA technique. Particularly, the linear response method seems to be the adequate tool for finite-temperature descriptions of collective vibrations in the presence of a very large number of pair configurations.

ACKNOWLEDGMENTS

This work was partially supported by the Comision de Investigationes (CIC) Pcia. de Bs. As., and by the Consejo Nacional de Investigaciones (CONICET) of Argentina.

[1]O. Civitarese, R. A. Broglia, and C. M. Dasso, Ann. Phys. (N.Y.) **156**, 412 (1984); R. A. Broglia, in *Nuclear Theory,* edited by G. F. Bertsch (World Scientific, Singapore, 1981), p. 94.
[2]D. Vautherin and N. Vinh Mau, Nucl. Phys. A **422**, 140 (1984).
[3]F. Alasia, O. Civitarese, and M. Reboiro, Phys. Rev. C **36**, 2555 (1987).
[4]W. Besold, P. G. Reinhard, and C. Toepffer, Nucl. Phys. A **431**, 1 (1984).
[5]J. Bar-Tour, Phys. Rev. C **32**, 1369 (1985).
[6]A. K. Kerman, S. Levit, and T. Troudet, Ann. Phys. (N.Y.) **148**, 436 (1983); A. K. Kerman and T. Troudet, *ibid.* **154**, 456 (1984); T. Troudet, Nucl. Phys. A **441**, 676 (1985).
[7]H. M. Sommermann, Ann. Phys. (N.Y.) **151**, 163 (1983).
[8]G. F. Bertsch, P. F. Bortignon, and R. A. Broglia, Rev. Mod. Phys. **55**, 287 (1983).
[9]P. Ring and P. Shuck, *The Nuclear Many-Body Problem* (Springer-Verlag, New York, 1980), pp. 314–319.
[10]O. Civitarese, S. Furui, M. Plotsajzack, and A. Faessler, Nucl. Phys. A **408**, 61 (1983).
[11]D. R. Bes, R. A. Broglia, and B. S. Nilsson, Phys. Rev. C **16**, 1 (1975).
[12]A. Bohr and B. R. Mottelson, *Nuclear Structure* (Benjamin, New York, 1969), Vol. I, pp. 81–83.
[13]S. G. Nilsson *et al.*, Nucl. Phys. A **131**, 1 (1969).
[14]O. Civitarese, G. G. Dussel, and R. P. J. Perazzo, Nucl. Phys. A **404**, 15 (1983).
[15]O. Civitarese, computer code RPAPH, Niels Bohr Institute.
[16]A. Bohr and B. R. Mottelson, *Nuclear Structure* (Benjamin, New York, 1975), Vol. II, pp. 607–615.